Journal of Materials Processing Technology 214 (2014) 962–968

Contents lists available at ScienceDirect

Journal of Materials Processing Technology

journal homepage: www.elsevier.com/locate/jmatprotec

Adaptive control of deposited height in GMAW-based layer additive manufacturing

Jun Xiong, Guangjun Zhang*

State Key Laboratory of Advanced Welding and Joining, Harbin Institute of Technology, Harbin 150001, China

ARTICLE INFO

Article history:
Received 18 August 2013
Received in revised form
11 November 2013
Accepted 11 November 2013
Available online 19 November 2013

Keywords:
Additive manufacturing
GMAW
Layer height
Adaptive control
Passive vision

ABSTRACT

A passive vision sensor system has been developed to monitor the nozzle to the top surface distance (NTSD) in layer additive manufacturing (LAM) using gas metal arc welding (GMAW). The deviations in the NTSD are compensated by the movement of the working flat, and the adjustment of the deposition rate on next deposition layer. After simplification of the controlled process into a linear system, an adaptive control system has been designed to keep the NTSD constant. The effectiveness of the controller is evaluated through deposition of single-bead multi-layer walls, and the experimental results confirm that the process stability can be improved when applying the developed controller.

1. Introduction

Layer additive manufacturing (LAM) is a progressive technique for fabricating complex components layer by layer with great potential of decreased time and minimum materials waste (Santos et al., 2006), in comparison to traditional subtractive manufacturing technologies. In this field, the weld-based LAM, using wire as the additive material, has gained lots of attentions due to a cleaner environment, a higher material saving, and a less risk of contamination (Heralic et al., 2012), as opposed to using power as the additive material. Martina et al. (2012) studied technological characteristics of plasma arc deposition for manufacturing of Ti-6Al-4V components. Based on the wire additive manufacturing, Baufeld et al. (2011) compared the mechanical and microstructure properties of Ti-6Al-4V objects built by laser and gas tungsten arc welding (GTAW) method, respectively. Xiong et al. (2009) developed a new approach, combining plasma arc deposition and milling technique, to improve the surface quality and dimensional accuracy of the parts.

Compared with other weld-based LAM methodologies, LAM using gas metal arc welding (GMAW) has shown great promises due to advantages including high productivity, low cost, and powerful bonding strength of components (Mughal et al., 2006). The research of the GMAW-based LAM has been widely explored, e.g. microstructure and mechanical properties of formed components (Spencer et al., 1998), the feasibility of using GMAW technology for building three-dimensional geometry (Zhang et al., 2003), and improvement of surface quality by means of mill technique (Karunakaran et al., 2010).

During the GMAW-based multi-layer deposition process, the work flat is lowered with a predefined layer height when a layer is deposited. A critical issue is that the deposited bead height is not always equal to the setting height. The reason can be attributed to the high sensitivity of the GMAW process to slight changes in deposition parameters, such as the arc current, deposition rate, arc voltage. Moreover, the layer geometry is related to the heat emission conditions at different layers, interlayer temperatures, surface quality of previous layers, and deformation of the base plate.

Thus, an accumulated error of layer height increases during multi-layer depositions. That is to say, the distance between the welding nozzle and the surface of the top layer is invariably changeable. It is well known that a long distance may generate bad gas protective effects, resulting in porosities or bad formation of the layer. In contrast, a short distance makes welding spatters adhere to the nozzle, or even a knock between the nozzle and the top surface of the layer. It is essential to monitor and control the nozzle to the top surface distance (NTSD) in real-time. To our knowledge, reliable and accurate control schemes for the layer height have not yet been fully developed in weld-based LAM. Doumanidis and Kwak (2002) employed structured-light vision

* Corresponding author at: State Key Laboratory of Advanced Welding and Joining, Harbin Institute of Technology, No. 92, West Da-Zhi Street, Harbin, Heilongjiang 150001, China. Tel.: +86 451 86415537; fax: +86 451 86415537.
E-mail addresses: zhanggj@hit.edu.cn, changfeng0007@163.com (G. Zhang).

0924-0136/$ – see front matter © 2013 Elsevier B.V. All rights reserved.
http://dx.doi.org/10.1016/j.jmatprotec.2013.11.014

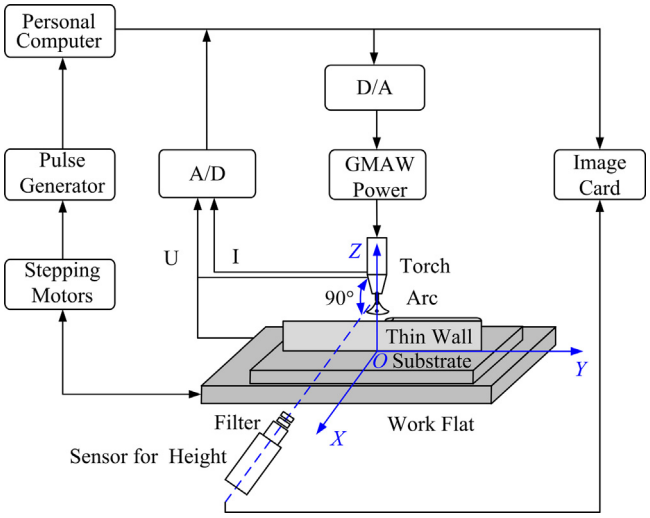

Fig. 1. Schematic diagram of GMAW-based LAM system.

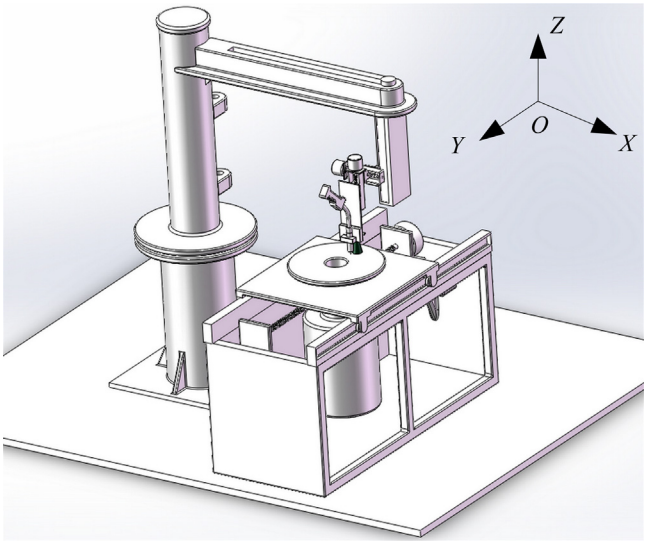

Fig. 2. Schematic diagram of work flat.

sensors for bead geometry measurement, and designed a one step ahead adaptive control system for geometry control. Heralic et al. (2010) developed a feed-forward compensator for the bead height using a laser vision sensor for detection. Nevertheless, a large lag or lead distance of the laser vision sensor always exists, increasing difficulties for control of the system.

The bead width in multi-layer deposition process has been kept consistent in our previous study (Xiong et al., 2013). This work aims at keeping the NTSD constant in GMAW-based LAM using a passive vision sensor. A closed-loop control of the deposited heights was established based on an adaptive controller. The effectiveness of the controller was evaluated through deposition of thin walls.

2. System overview

2.1. Experimental system

Fig. 1 illustrates the hardware of the GMAW-based LAM system, which mainly includes four parts, namely, a GMAW deposition power supply, a moveable and rotatable work flat, a passive vision sensor system, and a computer. The computer is the center of the control system. It is responsibility to implement several functions: control of the movement of the work flat using a data acquisition card, image display and processing, arc on/off control, adjustment of arc current and voltage, and human–machine interface designed to provide the user with all necessary information. It is noted that the work flat, driven by 3 independent stepping motors, has 3° of freedom including moving in the *Y*-axis or *X*-axis, and rotating around the *Z*-axis. The mechanical part of the work flat is simply presented in Fig. 2. During the multi-layer deposition process, the welding gun is always stationary, and the work flat is lowered after a layer is deposited.

2.2. Vision sensor design and image processing

Owing to the variable NTSD in multi-layer deposition process, it should be monitored and controlled in real-time. Thus, a passive vision sensor system is designed to observe the NTSD directly. As shown in Fig. 3, the vision sensor is placed opposite the welding nozzle. It consists of a CCD camera, a narrow-band and neural filter. The narrow-band filter was centered at 650 nm. With the appropriate aperture of the CCD camera, a perfect bead image can be acquired.

Fig. 4 displays the procedure of image processing for deposited bead height in GMAW-based LAM. Corresponding image processing algorithms, such as Gaussian filter, Sobel operator, and Hough transformation, were used to extract the characteristic information in the image, as seen in Fig. 4. The resolution of the image processing in the *Z*-axis is approximately 0.0625 mm/pixel. It is noteworthy that the nearly solidified region near the molten pool tail was set as the detection area, which is about 18 mm away from the wire electrode. This can not only ensure a solidified bead, but also obtain a less lag distance in comparison to 25.4 mm produced by the active vision sensor (Doumanidis and Kwak, 2002).

3. System identification

The objective of this study is to develop a controller for keeping the NTSD constant in GMAW-based LAM. The arc current, arc voltage, and deposition rate are three important process parameters. Among these main parameters, the deposition rate has most obvious effect on the deposited layer height (Xiong et al., 2012). Therefore, the control input is the deposition rate while the control output is the NTSD. To design a reliable controller, it is essential to understand and establish a precise dynamic model expressing the relationship between the system input and output.

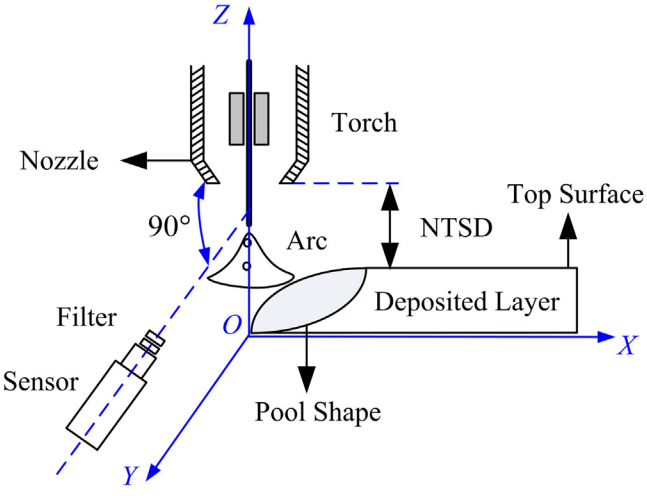

Fig. 3. Schematic of vision sensor system.

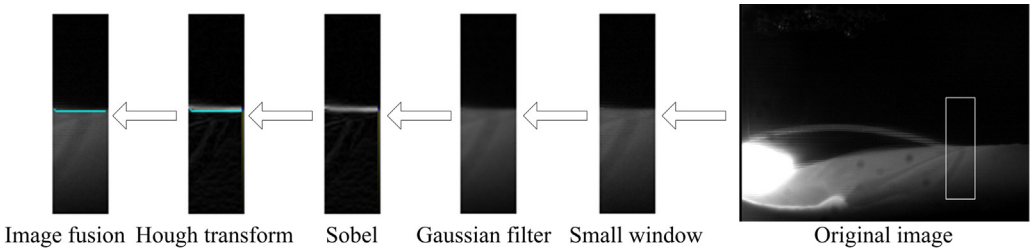

Fig. 4. Procedure of image processing for deposited layer height.

Table 1
Experimental condition of GMAW-based LAM.

Parameter	Value
Arc current	170 A
Arc voltage	23 V
Initial deposition rate	6 mm/s
Wire electrode diameter	1.2 mm
Ar (95%) and CO_2 (5%) gas flow	18 L/min
Size of mild steel substrate	260 mm × 80 mm × 9.5 mm

At first, step response experiments were performed to investigate the dynamic characteristics of the deposition process. This was achieved by applying a step change in the deposition rate, and the process was studied by recording the response of the single layer height. Other experimental conditions are shown in Table 1. As seen in Fig. 5, the response of the layer height is free of overshoot, and the process dynamics can be approximated with a first order transfer function expressed by Eq. (1).

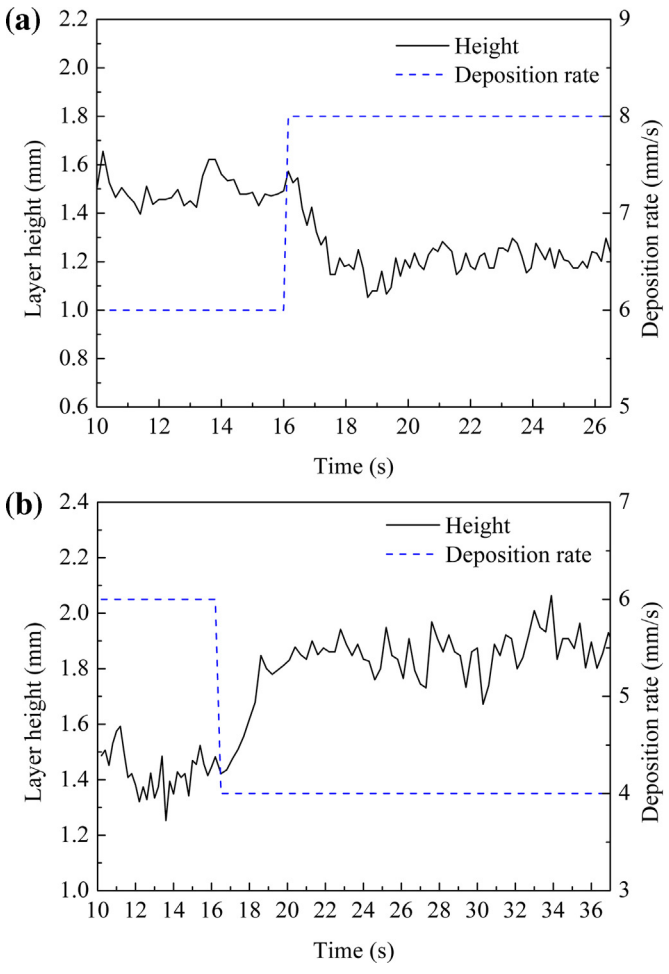

Fig. 5. Transient response of layer height to deposition rate. (a) Positive step and (b) negative step.

Table 2
Transfer function model coefficients with deposition rate step.

Positive step	K	−0.1524
	T_s	0.4760
	T_d	0.15
Negative step	K	−0.2192
	T_s	0.7519
	T_d	0.6

$$G(s) = \frac{K}{1+T_s} e^{-sT_d} \tag{1}$$

where K is the static gain, T_s is the time constant, and T_d is the time-delay constant.

The coefficients of the transfer function models are presented in Table 2. It is seen that time-delay always exists and changes. The corresponding coefficients of both models are different. At different stages in the deposition process, simple step responses cannot accurately represent the dynamic behavior.

Considering that a complex model is not beneficial to design and debug the controller. Therefore, a controlled autoregressive moving average model is applied to simulate the process. The structure of this model is expressed as:

$$A(z^{-1})y(k) = B(z^{-1})u(k-d) + e(k) \tag{2}$$

$$\begin{cases} A(z^{-1}) = 1 + a_1 z^{-1} + a_2 z^{-2} + \ldots + a_{n_a} z^{-n_a} \\ B(z^{-1}) = b_0 + b_1 z^{-1} + b_2 z^{-2} + \ldots + b_{n_b} z^{-n_b} \end{cases} \tag{3}$$

where $y(k)$ is the NTSD, $u(k)$ is the deposition rate, z^{-1} is the delay operator, n_a, n_b, and d are structural parameters, $e(k)$ is the white noise, $a_1, a_2, \ldots, a_{n_a}$ and $b_1, b_2, \ldots, b_{n_b}$ are coefficients of $A(z^{-1})$ and $B(z^{-1})$, respectively.

In order to obtain input–output data for the system identification, several deposition experiments were conducted using a range of different deposition rates. To simulate the special radiating structure of the deposition process, single-bead multi-layer depositions were conducted on the side of the substrate. Fig. 6 is given as a typical experiment. To obtain input data with persistent excitation to the dynamic process, the deposition rate is changed in a more

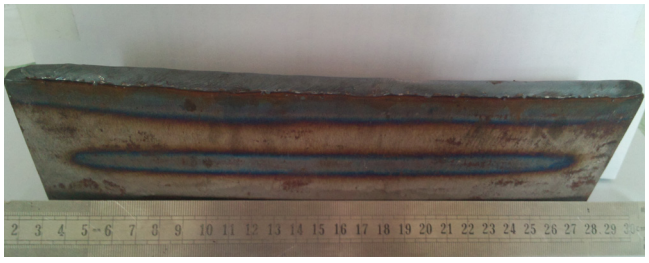

Fig. 6. An experimental sample using random deposition rate.

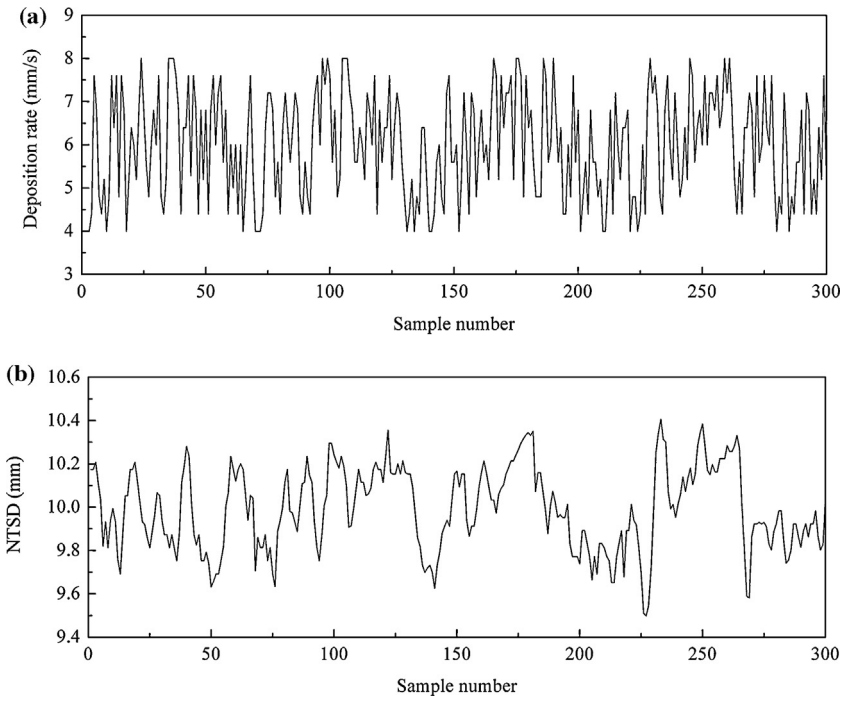

Fig. 7. Experimental transient response of the deposition process using a random deposition rate. (a) Deposition rate and (b) NTSD.

random way, as seen in Fig. 7(a). The system input is limited to 4–8 mm/s. The sampling period is 0.5 s, which is determined by the response time estimated from Fig. 5. The corresponding NTSD is shown in Fig. 7(b).

Based on the input–output data, and using the recursive least squares algorithm for system identification (Ljung, 1999), the structural parameters of the dynamic difference model can be calculated and selected as $n_a = 3$, $n_b = 3$, $d = 2$. Consequently, the delay of the deposition process is about 1.0 s. Fig. 8 presents the identified model response compared with the experimental output data. The output of the identified model is in good agreement with the actual output.

4. Controller design

Compared with the conventional welding process, the GMAW-based LAM is a multi-layer deposition process. Heat accumulation, interlayer temperature, and surface condition of previous layers are inevitable disturbances. The parameters of the estimated model are time-varying. Controllers with fixed parameters may not obtain satisfactory control effect, e.g. the proportional integral differential (PID) controller. In this study, an adaptive controller, which is capable of on-line system identification of the process parameters and regulating the parameters of the controller, was developed for the NTSD control. Using the generalized minimum variance algorithm as the performance index, the adaptive controller is given as:

$$u(k) = \frac{-G(z^{-1})y(k)}{\Lambda + B(z^{-1})F(z^{-1})} \tag{4}$$

Denote $\Lambda = \lambda^2/b_0$.where λ is a weighting term of the control variable.

$F(z^{-1})$ and $G(z^{-1})$ are expressed as follows:

$$\begin{cases} F(z^{-1}) = 1 + f_1 z^{-1} + \ldots + f_{d-1} z^{-(d-1)} \\ G(z^{-1}) = g_0 + g_1 z^{-1} + \ldots + g_{n-1} z^{-(n-1)} \end{cases} \tag{5}$$

where $n = n_a - 1$.

Assuming that the structural parameters of the process model, determined in Section 3, are constant, the adaptive controller can also be written as:

$$u(k) = \frac{-g_0 y(k) - g_1 y(k-1) - g_2 y(k-2) - b_1 u(k-1) - b_2 u(k-2) - b_3 u(k-3)}{\Lambda + b_0} \tag{6}$$

where $g_0, g_1, g_2, b_0, b_1, b_2, b_3$ are calculated online using forgetting factor recursive least square estimator.

The adaptive control system for GMAW-based LAM is presented in Fig. 9. It is seen that the controller contains an inner and an outer loop. The inner loop is identical to the conventional feedback control. The vision sensor is applied to detect the NTSD in real-time. The input of the control system is the deviation between the reference and detection value, and the output is the deposition rate. The outer loop consists of on-line identification of the process parameters and adjustment of the controller parameters.

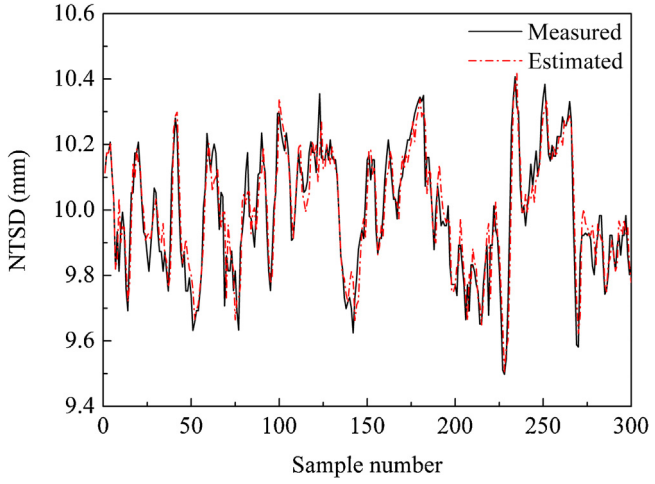

Fig. 8. Validation of the developed model using experimental output.

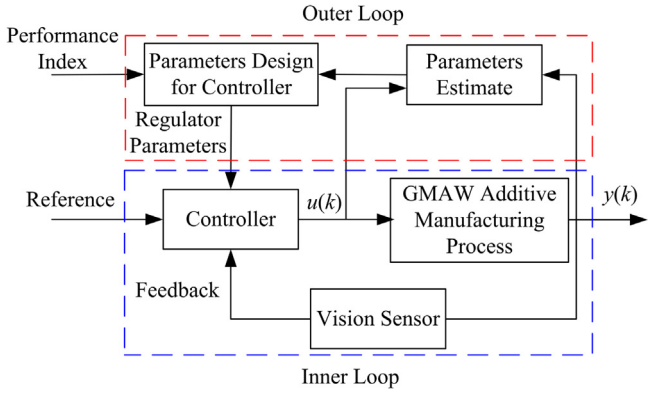

Fig. 9. Schematic diagram of adaptive controller for NTSD.

5. Experimental results

The reliability of the adaptive controller should be verified by experiments. In the future, our aim is to fabricate single-bead multi-layer components. Thus, two kinds of experiments, including open-loop and closed-loop control, were conducted through deposition of thin walls.

During the experiments, the welding gun was static, and the walls were generated by moving the work flat along a straight line. At the end of each layer the arc was turned off. The work flat was then moved to the initial position of the wall and lowered with a preset layer height. The arc was then turned on and a new layer was deposited.

First of all, a 21-layered wall with constant deposition rate (6 mm/s) was deposited. Other deposition parameters are shown in Table 1. Fig. 10 shows the detected NTSD of different layers. H_m and H_{set} are the detected and setting NTSD. It is noted that during the open-loop control experiments, the predefined layer height was 1.5 mm determined by experiences. That is to say, after each layer was deposited, the work flat was lowered by 1.5 mm. Arc starting and stopping points are not given in Fig. 10. The sampling period in Fig. 10 is 0.5 s. It is observed that with increasing the number of deposited layers, the deviation between the measured and set value increases. The left side of the curve is close to the arc starting points, and the right is close to the arc stopping points. Due to a high layer height at the arc starting points and a low layer height at the arc stopping points, the NTSD is increased gradually with all layers deposited in the same direction.

Another 21-layered wall was also deposited using the developed adaptive controller. The NTSD was the controlled variable, and the deposition rate was the control variable. Other process parameters were shown in Table 1. As can be seen in Table 2, the static gain of the transfer function is small. To avoid large deviations resulting in a too large deposition rate, the weighting term λ was set as large as possible. This can also prevent a large fluctuation of the bead width.

During the closed-loop control experiments, when one layer was deposited, the detected NTSD values were averaged. The work flat was lowered by the difference between 11.5 and the average value. The detected NTSD and corresponding deposition rate are presented in Fig. 11. The measured NTSD values fluctuate around the set value. Deviations, decreased obviously compared with that shown in Fig. 10, can be approximately limited to [−0.5, 0.5]. However, as shown in Fig. 11(d), the control accuracy deteriorates at the top layer. The reason is that a high layer height at the arc starting points and a low layer height at the arc stopping points always exist in a single deposition bead. With the increase in the number of layers, the height deviation between the arc starting and stopping points increases. Thus, the beginning and ending of the control points will also be influenced. In this case, the NTSD in these points

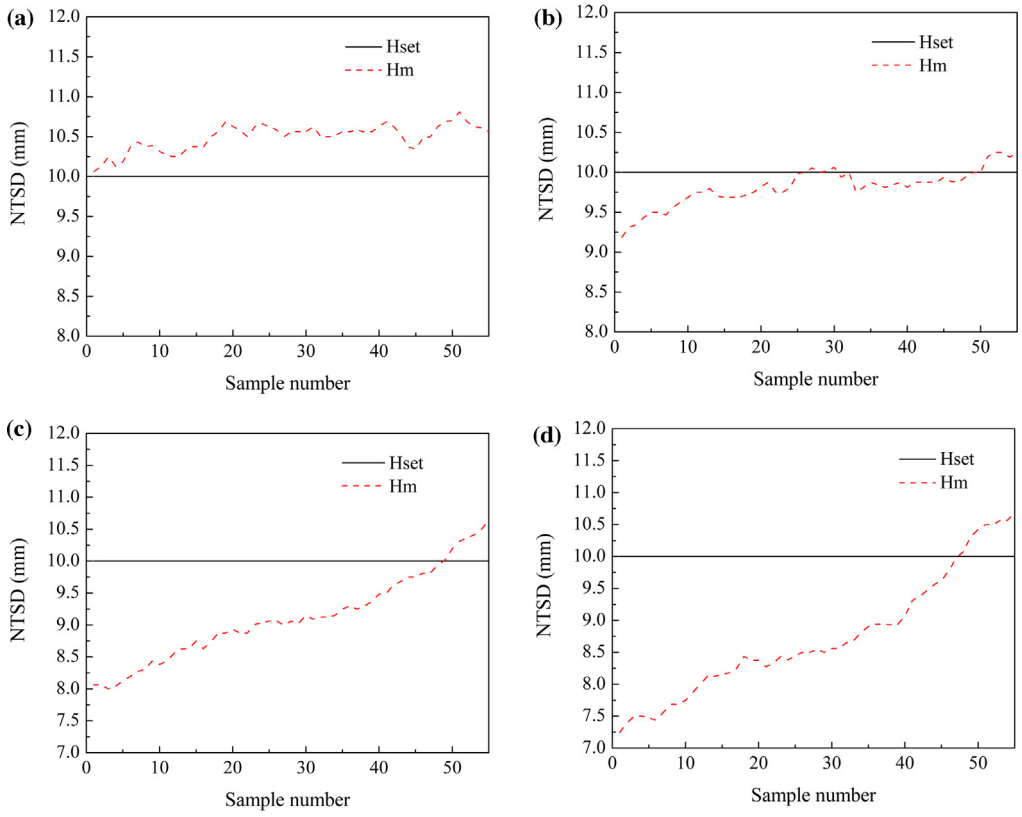

Fig. 10. NTSD measurements of various layers for the 21-layered wall. (a) Third layer, (b) ninth layer, (c) 15th layer and (d) 21st layer.

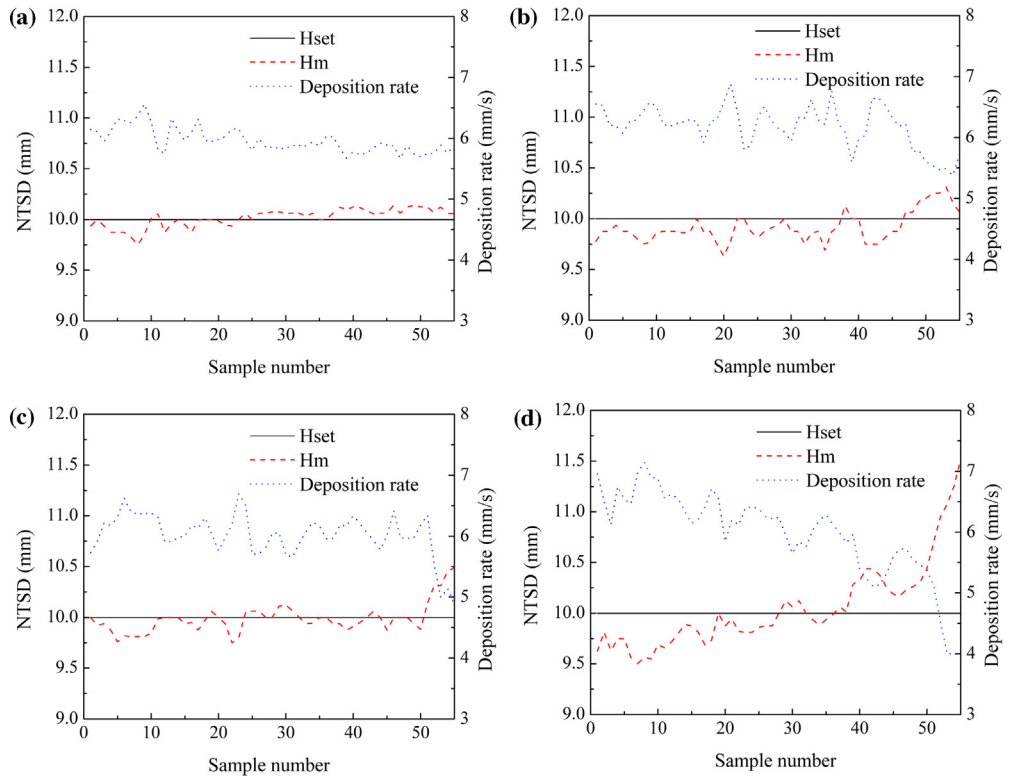

Fig. 11. Adaptive control results of different layers. (a) Third layer, (b) ninth layer, (c) 15th layer and (d) 21st layer.

cannot be kept constant with the adaptive controller, in which the deposition rate is adjusted in a limited range. New control strategies for arc starting and stopping points need to be developed. For instance, this can be avoided by fabricating closed path components, e.g. the cylinder. Control strategies for unclosed parts can also be applied, e.g. increasing deposition rate and arc current from upper values to the normal values gradually at arc starting points. For arc stopping points, the deposition rate and arc current can be decreased from normal values. Photographs of the deposited walls are shown in Fig. 12. The beginning of the control point is indicated by a vertical line.

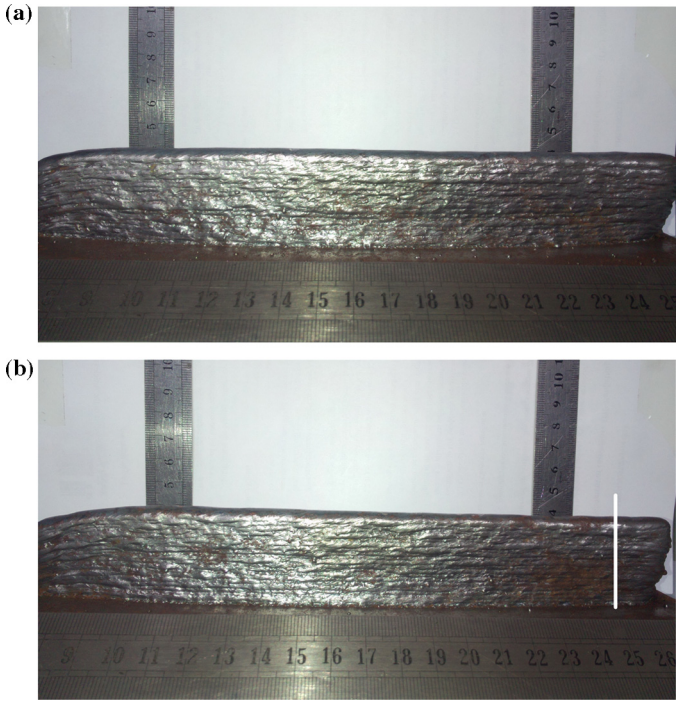

Fig. 12. Single-bead multi-layer walls. (a) Open-loop control and (b) closed-loop control.

6. Conclusion

A passive vision sensor system, and a process controller for layer height have been developed and estimated through deposition of single-bead multi-layer walls in GMAW-based LAM. The major conclusions are generalized as follows.

- The passive vision sensor is effective for monitoring the nozzle to the top surface distance. Clear deposition bead images are obtained.
- Image processing algorithms, including Gaussian filter, Sobel operator, and Hough transformation, were proposed to accurately extract the NTSD in the image.
- An adaptive controller by means of adjusting the deposition rate is introduced to keep the NTSD constant. The precision range of the control system is limited within ±0.5 mm.
- New control strategies for arc starting and stopping points need to be developed to eliminate the height deviation.

Acknowledgment

This work was supported by National Natural Science Foundation of China, No. 51175119.

References

Baufeld, B., Brandl, E., van der Biest, O., 2011. Wire based additive layer manufacturing: comparison of microstructure and mechanical properties of Ti-6Al-4V components fabricated by laser-beam deposition and shaped metal deposition. J. Mater. Process. Technol. 211, 1146–1158.

Doumanidis, C., Kwak, Y.M., 2002. Multivariable adaptive control of the bead profile geometry in gas metal arc welding with thermal scanning. Int. J. Pres. Ves. Pip. 79, 251–262.

Heralic, A., Christiansson, A.K., Ottosson, M., Lennartson, B., 2010. Increased stability in laser metal wire deposition through feedback from optical measurements. Opt. Lasers Eng. 48, 478–485.

Heralic, A., Christiansson, A.K., Lennartson, B., 2012. Height control of laser metal-wire deposition based on iterative learning control and 3D scanning. Opt. Lasers Eng. 50, 1230–1241.

Karunakaran, K.P., Suryakumar, S., Pushpa, V., Akula, S., 2010. Low cost integration of additive and subtractive processes for hybrid layered manufacturing. Robot. Comput. Integr. Manuf. 26, 490–499.

Ljung, L., 1999. System Identification: Theory for the User. Prentice Hall, Englewood Cliffs, NJ.

Martina, F., Mehnenb, J., Williams, S.W., Colegrove, P., Wanga, F., 2012. Investigation of the benefits of plasma deposition for the additive layer manufacture of Ti-6Al-4V. J. Mater. Process. Technol. 212, 1377–1386.

Mughal, M.P., Fawad, H., Mufti, R.A., 2006. Three-dimensional finite-element modelling of deformation in weld-based rapid prototyping. Proc. Inst. Mech. Eng. C: J. Eng. Mech. Eng. Sci. 220, 875–885.

Santos, E.C., Shiomi, M., Osakada, K., Laoui, T., 2006. Rapid manufacturing of metal components by laser forming. Int. J. Mach. Tools Manuf. 46, 1459–1468.

Spencer, J.D., Dickens, P.M., Wykes, C.M., 1998. Rapid prototyping of metal parts by three-dimensional welding. Proc. Inst. Mech. Eng. B: J. Eng. Manuf. 212, 175–182.

Xiong, X.H., Zhang, H.O., Wang, G.L., 2009. Metal direct prototyping by using hybrid plasma deposition and milling. J. Mater. Process. Technol. 209, 124–130.

Xiong, J., Zhang, G.J., Hu, J.W., Wu, L., 2012. Bead geometry prediction for robotic GMAW-based rapid manufacturing through a neural network and a second-order regression analysis. J. Intell. Manuf., http://dx.doi.org/10.1007/s10845-012-0682-1.

Xiong, J., Zhang, G.J., Qiu, Z.L., Li, Y.Z., 2013. Vision-sensing and bead width control of a single-bead multi-layer part: material and energy savings in GMAW-based rapid manufacturing. J. Clean Prod. 41, 82–88.

Zhang, Y.M., Chen, Y.W., Li, P.J., Male, A.T., 2003. Weld deposition-based rapid prototyping: a preliminary study. J. Mater. Process. Technol. 135, 347–357.